

alftoning on the wavelet domain

Maya R. Gupta

Ricoh California Research Center Menlo Park CA 94025 USA

ABSTRACT

Wavelet representations of images are increasingly important as more image processing functions are shown to be advantageously executed in the wavelet domain. Images may be inverse halftoned, compressed, denoised, and enhanced in the wavelet domain. In conjunction with other wavelet processing, it would be efficient to halftone directly from the wavelet domain. In this paper we demonstrate how to perform error diffusion in the wavelet domain. The wavelet coefficients are modified by a normalization factor and re-arranged. Then, traditional feed-forward raster scan error diffusion is performed and quality halftones are shown to result. Error diffusing in the wavelet domain is noted to be non-causal with respect to the pixels, and thus the method is not reproducible by feed-forward raster scan error diffusion of pixels. It is shown that the wavelet halftones preserve the average value of the input for constant patches. The resulting halftones may appear smoother in smooth regions and sharper at edges than the corresponding pixel-domain halftones. Disadvantages may include a greater susceptibility to moire and false contouring. Error diffusion is a two-dimensional sigma-delta modulation, and the ideas presented may also be useful for one-dimensional sigma-delta modulation applications.

Keywords: wavelets, wavelet domain, error diffusion, JPEG2000

1 INTRODUCTION

Wavelet representations of images are increasingly important as more image processing functions are shown to be advantageously executed in the wavelet domain. In this paper, we show how halftoning may be performed directly on the wavelet domain. In conjunction with other wavelet processing, such as JPEG2000 image compression or wavelet image enhancement, more efficient implementations may be possible by performing the halftoning without fully inverting the transform. Also, the wavelet domain error diffusion algorithm presented is non-causal, and thus is not reproducible by causal pixel domain error diffusion. Thus, the technique presented is novel and may lead to higher quality halftones, or halftones better suited for printing needs.

Error diffusion is a common halftoning technique that has been the topic of much research in the last twenty-five years. A good review of error diffusion research can be found in Kang's book on digital halftoning.¹

In this paper, we show that it is possible to perform error diffusion directly on the two-dimensional wavelet domain in order to produce a visually pleasing halftone and possibly achieve more efficient processing in combination with other wavelet methods such as JPEG2000. Wavelet basics are reviewed, and other research combining wavelets and halftoning is examined. Then, the wavelet domain error diffusion algorithm is presented. The dc-preserving property of pixel-domain error diffusion is shown to hold, and example halftones are given.

2 WAVELETS

Wavelets are a compromise between the time domain and the Fourier domain, allowing simultaneous resolution in both time and frequency. Wavelet research and applications exploded in the last decade, showing that working in the wavelet domain could be useful in image compression,² image denoising,³ image enhancement,⁴ and inverse halftoning,⁵ as well other image processing tasks. As more of the document processing pipeline moves to the wavelet domain, it would be more efficient to be able to also halftone directly on wavelet coefficients.

Further author information: Send correspondence to Maya R. Gupta)
Maya R. Gupta: E-mail: mgupta@rii.ricoh.com, Telephone: 650)496-5735

Wavelet coefficients represent averages and differences of the time(spatial) domain signal at different resolutions. Wavelet coefficients can be computed by a low-pass and high-pass filterbank, with one filterbank per resolution level. A good resource about wavelets for researchers with a signal processing background is *Wavelets and Subband Coding*.⁶ Notation in this paper is based on the book by Mallat.⁷

A one-dimensional wavelet transform decomposes an input signal x with scaled and shifted versions of a (lowpass) scaling function ϕ and (highpass) wavelet ψ .

A two-dimensional separable wavelet transform first converts a pixel domain image into four subband images: a low-pass filtering in both directions, a low-pass filtering in one direction and high-pass in the other direction, vice-versa, and a high-pass filtering in both directions. Each subband image is down-sampled by a factor of 2 in each direction and is termed (respectively) a_1, d_1^1, d_1^2, d_1^3 . Then the lowpass subband image a_1 is further decomposed into four higher level subband images, which are downsampled by 2 in each direction and termed, a_2, d_2^1, d_2^2 and d_2^3 . The process is repeated until the desired resolution level is achieved. The end result of a j level multiresolutional decomposition of a $N \times N$ image is a $2^{-j}N \times 2^{-j}N$ lowpassed image a_j and three difference images for each of the j levels, where the difference images at level j are size $2^{-j}N \times 2^{-j}N$.

3 RELATED RESEARCH IN WAVELETS AND HALFTONING

A number of authors have considered combining multiresolutional ideas with halftoning. One category of such work was spearheaded by Ping Wah Wong and includes work by Wong⁸ and Goldschneider et al.⁹ These two papers investigate the problem of designing an error diffused image that can be rendered with good image quality at many different resolutions. The actual halftoning is, however, done in the pixel domain.

Another category of work^{1, 11} create halftones such that the energy of each multiresolutional level in the halftone matches the energy of that multiresolutional level of the original image. These halftoning algorithms directly minimize the error between the multiresolutional averages of the original image and halftone at all resolutions. Similarly, block color quantization halftoning¹² minimizes the distortion between small blocks in the input image and corresponding blocks in the output image.

Katsavoundidis and Kuo also proposed a goal of mean-matching between the original image and the halftone image in their papers^{13, 14} but their algorithms are variations on error diffusion. In the earlier paper,¹³ the pixels are quantized in a random scan order. Error is diffused symmetrically after a pixel is quantized, as opposed to the traditional forward-only error propagation step. Since the scan order is random, some neighboring pixels may already be quantized, in which case the error that would have been passed to them is instead summed into a 'global error' for that local region. 'Global errors' are passed to neighboring regions using the same spatial error filter. Thus they propose the idea of passing some error from different regions within a scale. A modified algorithm by the same authors¹⁴ has a nonlinear but non-random scanning order of the pixels, quantizes pixels, and uses a non-causal filter (due to the nonlinear scan order). For that algorithm the multiresolutional framework only affects the scan order of the pixels.

Lastly, an adaptive screen for dithering¹⁵ has been proposed in which the information about how to adapt the dither screen is pulled from the wavelet transform representation.

The algorithm presented in this paper uses traditional feed-forward raster-scan error diffusion on wavelet transform coefficients to create a binarized image.

4 WAVELET DOMAIN ERROR DIFFUSION ALGORITHM AND SOME PROPERTIES

Given a wavelet transform image, we outline how to re-arrange the transform coefficients, scale them appropriately, and then perform traditional feed-forward raster-scan error diffusion on the wavelet transform coefficients in order to create a binarized image. There is no need to take an inverse wavelet transform. One way to interpret the algorithm is to view the multiresolutional representation as a downsampled image (the lowest resolution) with directional errors (the difference or wavelet coefficients). The downsampled image coefficient steers the error diffusion to the correct local average value, and the difference coefficients provide local corrections.

Step 1: For a $N \times N$ image, interweave the wavelet transform coefficients of the different subband images. For a j level wavelet transform, replace each $2^j \times 2^j$ block by the average and difference coefficients associated with the pixel in the upper left of the pixel block.

For example, for a one-level multiresolutional transform (which consists of lowpass image a_1 and difference images d_1, d_2, d_3), arrange the wavelet transform coefficients as follows:

$$\begin{array}{cccccc} a_1[1, 1] & d_1^1[1, 1] & a_1[1, 2] & d_1^1[1, 2] & a_1[1, 3] & d_1^1[1, 3] \\ d_1^2[1, 1] & d_1^3[1, 1] & d_1^2[1, 2] & d_1^3[1, 2] & d_1^2[1, 3] & d_1^3[1, 3] \\ a_1[2, 1] & d_1^1[2, 1] & a_1[2, 2] & d_1^1[2, 2] & a_1[2, 3] & d_1^1[2, 3] \\ d_1^2[2, 1] & d_1^3[2, 1] & d_1^2[2, 2] & d_1^3[2, 2] & d_1^2[2, 3] & d_1^3[2, 3] \\ \vdots & & & & & \end{array} \quad (1)$$

For a two-level multiresolutional transform, we arranged the coefficients as follows:

$$\begin{array}{cccccc} a_2[1, 1] & d_1^1[1, 1] & d_2^2[1, 1] & d_1^1[1, 2] & a_2[1, 2] & d_1^1[1, 3] \\ d_1^2[1, 1] & d_1^3[1, 1] & d_1^2[1, 2] & d_1^3[1, 2] & d_1^2[1, 3] & d_1^3[1, 3] \\ d_2^2[1, 1] & d_1^1[2, 1] & d_2^3[1, 1] & d_1^1[2, 2] & d_2^2[1, 2] & d_1^1[2, 3] \\ d_1^2[2, 1] & d_1^3[2, 1] & d_1^2[2, 2] & d_1^3[2, 2] & d_1^2[2, 3] & d_1^3[2, 3] \\ \vdots & & & & & \end{array} \quad (2)$$

Higher level transform coefficients should be arranged analogously.

Let $X[m, n]$ index the $N \times N$ image of re-arranged wavelet transform coefficients as shown above.

Step 2: Normalize the re-arranged wavelet transform coefficients for all m, n by a factor :

$$X'[m, n] = X[m, n] \quad (3)$$

where the factor ensures that the two-dimensional scaling function at scale j integrates to four, thus preserving the input dc-value in the halftone,

$$= \frac{4}{\phi_j(y)\phi_j(z)dydz} \quad (4)$$

where $\phi_j(y)$ is the one-dimensional scaling function for level j .

Step 3: Perform error diffusion on the normalized wavelet coefficients using the traditional error diffusion equations to create the output binary halftone $Q(\tilde{X}'[m, n])$:

$$Q(z) = \begin{cases} 1 & \text{if } z \geq 128, \\ 0 & \text{if } z < 128 \end{cases} \quad (5)$$

$$e[m, n] = \tilde{X}'[m, n] - Q(\tilde{X}'[m, n]) \quad (6)$$

$$\tilde{X}'[m, n] = X'[m, n] + \sum_{r=1}^R \sum_{s=1}^R h[r, s]e[m-r, n-s] \quad (7)$$

where the modified wavelet domain signal \tilde{X}' is the normalized wavelet domain signal X' plus an error signal e filtered by an R -tap filter h where $\sum_r \sum_s h[r, s] = 1$ and $h[r, s] \geq 0$ for all r, s . The modified input signal is quantized to create the output binary signal $Q(\tilde{X}')$.

Example: Consider an 8x8 image with pixel values [0,255] shown below:

$$\begin{array}{cccccccc}
 180 & 180 & 180 & 180 & 180 & 20 & 20 & 20 \\
 180 & 180 & 180 & 180 & 180 & 20 & 20 & 20 \\
 180 & 180 & 180 & 180 & 180 & 20 & 20 & 20 \\
 180 & 180 & 180 & 180 & 180 & 20 & 20 & 20 \\
 180 & 180 & 180 & 180 & 180 & 20 & 20 & 20 \\
 180 & 180 & 180 & 180 & 180 & 20 & 20 & 20 \\
 180 & 180 & 180 & 180 & 180 & 20 & 20 & 20 \\
 180 & 180 & 180 & 180 & 180 & 20 & 20 & 20
 \end{array} \tag{8}$$

Then the one level Haar transform, scaled and arranged as decreed in Step 1 ($n = 2$), is

$$\begin{array}{cccccccc}
 720 & 0 & 720 & 0 & 400 & 0 & 80 & 0 \\
 0 & 0 & 0 & 0 & 320 & 0 & 0 & 0 \\
 720 & 0 & 720 & 0 & 400 & 0 & 80 & 0 \\
 0 & 0 & 0 & 0 & 320 & 0 & 0 & 0 \\
 720 & 0 & 720 & 0 & 400 & 0 & 80 & 0 \\
 0 & 0 & 0 & 0 & 320 & 0 & 0 & 0 \\
 720 & 0 & 720 & 0 & 400 & 0 & 80 & 0 \\
 0 & 0 & 0 & 0 & 320 & 0 & 0 & 0
 \end{array} \tag{9}$$

After processing with the Floyd-Steinberg error diffusion filter, the modified input \tilde{X}' (the input wavelet domain signal plus the inherited error) to the quantizer is (rounded for visibility),

$$\begin{array}{cccccccc}
 720 & 203 & 697 & 194 & 373 & 52 & 103 & 45 \\
 136 & 44 & 143 & -19 & 355 & 86 & 81 & 56 \\
 691 & 176 & 649 & 178 & 413 & 117 & 173 & -13 \\
 121 & 130 & 49 & 52 & 409 & 99 & 22 & 0 \\
 734 & 187 & 708 & 246 & 466 & 137 & 42 & 20 \\
 137 & 42 & 154 & 21 & 372 & 35 & 25 & 20 \\
 691 & 178 & 661 & 200 & 421 & 96 & 135 & -45 \\
 122 & 132 & 58 & 65 & 414 & 88 & -1 & -22
 \end{array} \tag{10}$$

The error signal e is (rounded for visibility),

$$\begin{array}{cccccccc}
 465 & -52 & 442 & -61 & 118 & 52 & 103 & 45 \\
 -119 & 44 & -112 & -19 & 100 & 86 & 81 & 56 \\
 436 & -79 & 394 & -77 & 158 & 117 & -82 & -13 \\
 121 & -125 & 49 & 52 & 154 & 99 & 22 & 0 \\
 479 & -68 & 453 & -9 & 211 & -118 & 42 & 20 \\
 -118 & 42 & -101 & 21 & 117 & 35 & 25 & 20 \\
 436 & -77 & 406 & -55 & 166 & 96 & -120 & -45 \\
 122 & -123 & 58 & 65 & 159 & 88 & -1 & -22
 \end{array} \tag{11}$$

The resulting halftone is,

$$\begin{array}{cccccccc}
255 & 255 & 255 & 255 & 255 & 0 & 0 & 0 \\
255 & 0 & 255 & 0 & 255 & 0 & 0 & 0 \\
255 & 255 & 255 & 255 & 255 & 0 & 255 & 0 \\
0 & 255 & 0 & 0 & 255 & 0 & 0 & 0 \\
255 & 255 & 255 & 255 & 255 & 255 & 0 & 0 \\
255 & 0 & 255 & 0 & 255 & 0 & 0 & 0 \\
255 & 255 & 255 & 255 & 255 & 0 & 255 & 0 \\
0 & 255 & 0 & 0 & 255 & 0 & 0 & 0
\end{array} \tag{12}$$

One way to interpret the algorithm is to view the multiresolutional representation as a downsampled image (the lowest resolution) with directional errors (the difference or wavelet coefficients). The downsampled image coefficient steers the error diffusion to the correct local average value, and the difference coefficients provide local corrections.

As the number of multiresolutional levels goes up, more artifacts are introduced due to the multiresolutional representation, and a smoother looking halftone with more jagged edges results. Error diffusion filters generally do not have an extent greater than five or six taps in any direction.¹ Using high level wavelet transform coefficients means the error diffusion is being performed on transform coefficients that represent pixels that are relatively far away. Experiments show that the level should be limited so that the extent of the error diffusion filter and the spatial extent the pixel transform coefficients represent is not much larger than a well-designed traditional error diffusion filter's extent.

4 1 Noncausality

Feed-forward, raster scan error diffusion on the wavelet coefficients is fundamentally different than feed-forward raster scan error diffusion on the pixel domain. A key difference is that feed-forward raster scan error diffusion in the pixel domain is a causal algorithm. Error diffusing the wavelet coefficients is noncausal with respect to the pixel domain. For instance, a lowpass coefficient from the one level Haar transform contains information about the pixel to the right, down, and down-right of where that lowpass coefficient is located. Thus when the error diffusion quantizes that lowpass coefficient it is accessing future information about pixels it spatially has not yet reached. Therefore, traditionally causal error diffusion done directly on the pixel domain will not create the same result irrespective of error diffusion filter.

4 2 Moire

When two close frequencies are superimposed, an unwanted lower frequency 'beat' may result. This effect is called 'moire'. If the original image has a periodic structure (for example, if it has a regular cluster dot dither halftone structure already in it) then traditional error diffusion may lead to some moire. However, when error diffusion is done on the wavelet domain, there is a high frequency regular periodic structure from the arrangement of the wavelet transform coefficients. More periodicity before the halftoning means greater danger of moire. On unfiltered images of scanned cluster dot dithered gray patches at various cluster dot frequencies, some moire patterns occurred with the wavelet error diffusion at the first level. The moire was worse for error diffusion on the second level wavelet domain.

4 3 Error diffusion on the wavelet domain preserves dc value

Error diffusion is dc-preserving for filters h whose taps are all positive and sum to one ($\sum_r \sum_s h[r, s] = 1$). That is, for a constant input signal $x[j, k] = a$, the average of the quantized output signal will converge to a :

$$\lim_{m, n \rightarrow \infty} \frac{1}{MN} \sum_{m=1}^M \sum_{n=1}^N Q(\tilde{x}[m, n]) = a$$

Error diffusion preserves the input value average because all signal is quantized eventually, and no signal is introduced into the halftone that did not come from the original signal

Error diffusion on the wavelet domain, as described in section 4 also preserves the input value for constant patches:

Proposition: For a constant input signal $x[m, n] = a$ for all m, n , and finite-tap error diffusion filter with $h[r, s] \geq 0$ for all r, s and $\sum_r \sum_s h[r, s] = 1$, the average of the output of the algorithm outlined above will converge to a :

$$\lim_{M, N \rightarrow \infty} \frac{1}{MN} \sum_{m=1}^M \sum_{n=1}^N Q(\tilde{X}'[m, n]) = a \quad (13)$$

Proof: The proposition is proved for error diffusion on one-level wavelet transforms. The proof for higher levels is analogous.

The limit,

$$\lim_{M, N \rightarrow \infty} \frac{1}{MN} \sum_{m=1}^M \sum_{n=1}^N Q(\tilde{X}'[m, n])$$

Can be rewritten using equation 6,

$$\lim_{M, N \rightarrow \infty} \frac{1}{MN} \sum_{m=1}^M \sum_{n=1}^N (\tilde{X}'[m, n] - e[m, n])$$

Substituting from equation 7, the expression becomes

$$\lim_{M, N \rightarrow \infty} \frac{1}{MN} \sum_{m=1}^M \sum_{n=1}^N \left(X'[m, n] - e[m, n] + \sum_{r=1}^R \sum_{s=1}^S h[r, s] e[m-r, n-s] \right) \quad (14)$$

Since the input x is a constant patch, the high-pass wavelet coefficients are zero: $X[2m+1, 2n] = X[2m, 2n+1] = X[2m+1, 2n+1] = 0$ for all $m, n = 1, 2, \dots$. The $X[2m, 2n]$ are nonzero scaling coefficients. The scaling coefficients are computed as an inner product of the pixel domain signal and the shifted and scaled wavelet scaling function ϕ : $X[2m, 2n] = \langle x, \phi_{1-m} \phi_{1-n} \rangle$. Since the input signal is constant, $x[m, n] = a$ for all m, n . Then, $X[2m, 2n] = a \langle 1, \phi_{1-m} \phi_{1-n} \rangle$. Then, due to the normalization in equation 3, the normalized coefficient is $X'[2m, 2n] = 4a$. Then the limit can be re-written,

$$a \lim_{M, N \rightarrow \infty} \frac{1}{MN} \sum_{m=1}^{M/4} \sum_{n=1}^{N/4} 4 + \lim_{M, N \rightarrow \infty} \frac{1}{MN} \sum_{m=1}^M \sum_{n=1}^N \left(-e[m, n] + \sum_{r=1}^R \sum_{s=1}^S h[r, s] e[m-r, n-s] \right)$$

Changing back to the summation limits the expression is,

$$a \lim_{M, N \rightarrow \infty} \frac{1}{MN} \sum_{m=1}^M \sum_{n=1}^N 1 + \lim_{M, N \rightarrow \infty} \frac{1}{MN} \sum_{m=1}^M \sum_{n=1}^N \left(-e[m, n] + \sum_{r=1}^R \sum_{s=1}^S h[r, s] e[m-r, n-s] \right)$$

Next, expand the sum over all the input pixels,

$$\begin{aligned} a + \lim_{M, N \rightarrow \infty} \frac{1}{MN} & - e[m, n] + \sum_{r=1}^R \sum_{s=1}^S h[r, s] e[M-r, N-s] - e[m, n-1] \\ & + \sum_{r=1}^R \sum_{s=1}^S h[r, s] e[M-1-r, N-s] + \dots + e[0, 0] \end{aligned}$$

Expand the sum over the filter taps and re-group terms,

$$\begin{aligned}
a + \lim_{M, N \rightarrow \infty} \left(\frac{1}{MN} \right) &- e[M, N] + (h[1, 1] - 1)e[M - 1, N - 1] \\
&+ (h[1, 1] + h[1, 2] - 1)e[M - 1, N - 2] + (h[1, 1] + h[2, 1] - 1)e[M - 2, N - 1] \\
&+ (h[1, 1] + h[1, 2] + h[2, 1] + h[R, S] - 1)e[M - R, N - S] \\
&+ \left(\sum_{r=1}^R \sum_{s=1}^S h[r, s] - 1 \right) e[M - R - 1, N - S - 1] \\
&+ \left(\sum_{r=1}^R \sum_{s=1}^S h[r, s] - 1 \right) e[M - R - 1, N - S - 2]
\end{aligned}$$

Since $\sum_{r=1}^R \sum_{s=1}^S h[r, s] = 1$, the limit expression simplifies to the $R \times S$ terms of e ,

$$\begin{aligned}
a + \lim_{M, N \rightarrow \infty} \left(\frac{1}{MN} \right) &- e[M, N] + (h[1, 1] - 1)e[M - 1, N - 1] \\
&+ (h[1, 1] + h[1, 2] - 1)e[M - 1, N - 2] + (h[1, 1] + h[2, 1] - 1)e[M - 2, N - 1] \\
&+ (h[1, 1] + h[1, 2] + h[2, 1] + h[R, S] - 1)e[M - R, N - S + 1]
\end{aligned}$$

Since R, S are finite and absolute value $\|e[m, n]\| \leq 5$ for all m, n , the above limit is bounded below by,

$$\geq a + \lim_{M, N \rightarrow \infty} \frac{-5RS}{MN}$$

and upperbounded by,

$$\leq a + \lim_{M, N \rightarrow \infty} \frac{5RS}{MN}$$

Both the upper and lower bound evaluate to a , and thus we can conclude that,

$$\lim_{M, N \rightarrow \infty} \frac{1}{MN} \sum_{m=0}^M \sum_{n=0}^N Q(\tilde{X}[m, n]) = a$$

5 FILTER DESIGN

Designing filters for use in the wavelet domain may require different wisdom than designing filters for use in the pixel domain, but we expect and find that many of the tricks of filter design still hold, though perhaps to different degrees.

One of the keys to filter design is the extent of the filter. However, since wavelet transform coefficients represent a local region of pixels, an R tap filter in the wavelet domain is actually acting on many more than R pixels. The exact influence depends on the level of the wavelet transform and the extent of the wavelet transform filters.

Experimentation suggests that filters with relatively significant weight in the opposite of the raster scan direction helped ameliorate horizontal and vertical spatial frequency artifacts in the halftone. In the *Example Halftones* section, results are shown with the Shiao-Fan and Stucki filters.¹ which have, respectively, three and four taps to the left of the filtered coefficient.

Error diffusion researchers have optimized error diffusion filters for use in the pixel domain, a review of that literature is found in Kang's book on halftoning.¹ Similarly, a wavelet filter could be designed that minimized

(or aimed to minimize) a metric for visual artifacts, perhaps using a human visual system model in the fourier domain or perhaps the sCIELAB model^{16,17}

One might think to use different filters for each subband or each multiresolutional level. We did not find visually-pleasing results with using different filters for different subbands or levels. Error diffused halftones appear visually appealing because the majority of the halftoning artifacts are pushed to the high spatial frequencies where they are less visually notable. Changing filters for each subband led to visible noise and structural or ‘bias’ artifacts where edges move or have shadows in certain directions. However, further research may yield an advantage to subband or level adaptive filters.

Another idea is to pass the error at a level only to other coefficients of that same multiresolutional level. Theoretically, following the proof in section 4.3, one can see that the halftone will not maintain the correct average, as the lower level (low-pass) coefficients must diffuse error throughout the entire spatial area they represent in order to reproduce the correct image average in that area. In any given spatial area there are coefficients from different levels, thus restricting passed error to coefficients only of other levels creates halftones that cannot reproduce the correct average output for a constant input patch.

6 EXAMPLE HALFTONES

For the example halftones, we used the Haar wavelet transform or the reversible 5-3 filter (two-dimensions and separable) that is used in the JPEG2000 image compression standard,² with mirror-reflection at boundaries. The one-dimensional Haar or reversible 5-3 forward transform is applied to rows then columns of the image. The one-dimensional reversible 5-3 forward transform is given by,

$$X[2n+1] = x[2n+1] - \left\lfloor \frac{x[2n] + 2[2n+2]}{2} \right\rfloor \quad (15)$$

$$X[2n] = x[2n] + \left\lfloor \frac{X[2n-1] + X[2n+1] + 2}{4} \right\rfloor \quad (16)$$

for $n = 0, 1, 2, \dots$, where even transform coefficients $X[2n]$ are lowpass coefficients and odd transform coefficients $X[2n+1]$ are highpass coefficients.

The images were halftoned using the Stucki filter¹ and a filter from Shiau and Fan that was designed for simple implementation and its worm-reducing properties.¹

Stucki filter

			X	8/42	4/42
2/42	4/42	8/42	4/42	2/42	
1/42	2/42	4/42	2/42	1/42	

Shiau Fan filter

			X	8/16
1/16	1/16	2/16	4/16	

In figure 1, four different gray patches are printed with the two different filters. The patch values were drawn randomly from a uniform distribution on [0,255] and the values from left to right are 63, 14, 223, and 102. Similar results were seen with other filters, but the significant filter strength to the left of the filtered coefficient in the Stucki and Shiau-Fan filters ameliorated horizontal and vertical spatial frequency artifacts.

In figure 2, pixel domain and one-level reversible 5-3 wavelet domain error diffusion are contrasted. In figure 3, examples are presented with for the one-level Haar wavelet and for the two-level reversible 5-3.

The halftone images are very smooth in some regions, but this smoothness, as with dither, implies a greater risk of false contouring.

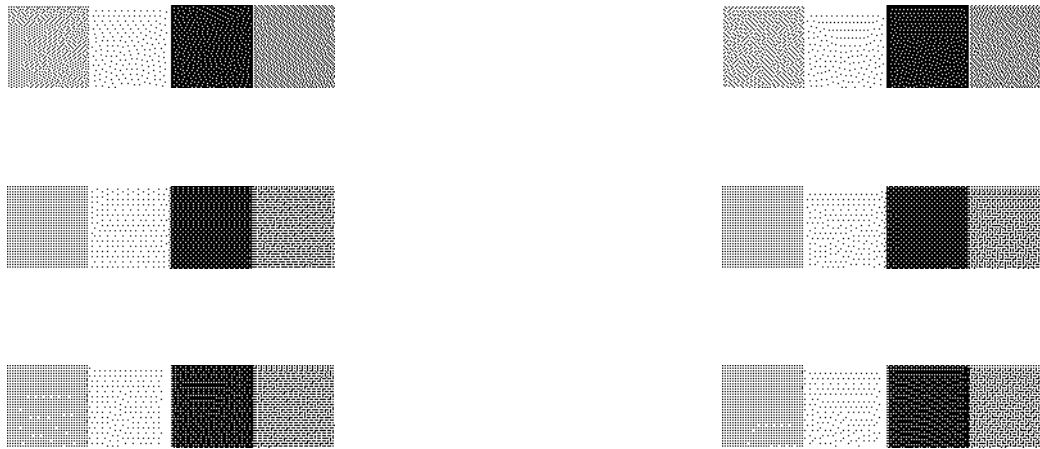


Figure 1 Top left: Shiau-Fan filter error diffusion on the pixel domain. Top right: Stucki filter error diffusion on the pixel domain. Middle left: Shiau-Fan filter error diffusion on the one-level Haar domain. Top right: Stucki filter error diffusion on the one-level Haar domain. Bottom left: Shiau-Fan filter error diffusion on the one-level reversible 5-3 wavelet domain. Bottom right: Stucki filter error diffusion on the one-level reversible 5-3 wavelet domain.

The halftones are printed at 1 bit at 75 dpi to minimize degradation in reproduction. To mimic the impression of a 600 dpi image at 1 ft viewing distance, the figures should be viewed at 8 ft viewing distance. Clearly, halftones actually printed at 600 dpi will have dots with a more rounded shape and that may affect image quality.

7 CONCLUSIONS

Wavelet representations of images are increasingly important as more image processing functions are shown to be advantageously executed in the wavelet domain. In this paper, we have shown that error diffusion may be performed directly on the wavelet domain. In conjunction with other wavelet processing, such as JPEG2000 image compression or wavelet image enhancement, more efficient implementations may be possible by performing the halftoning without fully inverting the transform.

Good visual quality with practical error diffusion filters has been shown for reversible 5-3 wavelet transform used in JPEG2000. At high dpi, traditional error diffusion still suffers from graininess. Results with wavelet halftones suggest that smoother results can be achieved.

Although the use of sigma-delta modulation in two dimensions (error diffusion) for halftoning is due to Floyd and Steinberg in 1975,¹⁸ one dimensional sigma-delta modulation dates back to at least the 60's.¹⁹ Perhaps the use of sigma-delta modulation on the wavelet domain would work well for one-dimensional applications, such as audio, as well.

7.1 Acknowledgments

The author would like to thank Anna Gilbert, Kathrin Berkner, and Martin Boliek for helpful comments and suggestions.

REFERENCES

1. H. Kang, *Digital Color Halftoning*, SPIE Optical Engineering Press, USA, 1999.
2. www.jpeg.org/JPEG2000.html.

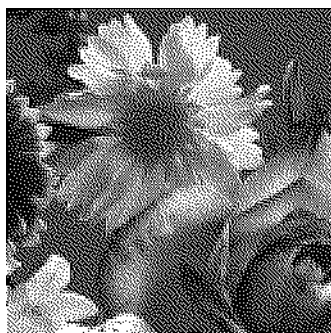


Figure 2 Top left: Shiau-Fan filter error diffusion on the pixel domain. Top right: Shiau-Fan filter error diffusion on the one-level reversible 5-3 wavelet domain. Bottom left: Stucki filter error diffusion on the pixel domain. Bottom right: Stucki filter error diffusion on the one-level reversible 5-3 wavelet domain.

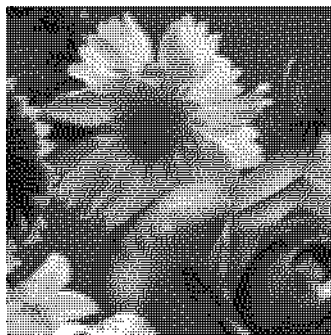


Figure 3 Top left: Shiau-Fan filter error diffusion on the one-level Haar domain. Top right: Shiau-Fan filter error diffusion on the two-level reversible 5-3 wavelet domain. Bottom left: Stucki filter error diffusion on the one-level Haar domain. Bottom right: Stucki filter error diffusion on the two-level reversible 5-3 wavelet domain.

3. D. L. Donoho, "De-noising by soft-thresholding, *IEEE Trans. on Information Theory* **41**(3), pp. 613–627, 1995.
4. K. Berkner, M. Gormish, and E. Schwartz, "Multiscale sharpening and smoothing in besov spaces with appliations to image enhancement, *Applied Computational and Harmonic Analysis* **11**, pp. 2–31, July 2001.
5. Z. Xiong, M. Orchard, and K. Ramchandran, "Inverse halftoning using wavelets, *IEEE Trans. on Image Proc.* **8**, pp. 1479–1483, October 1999.
6. M. Vetterli and J. Kovačević, *Wavelets and subband coding*, Prentice Hall Inc, USA, 1995.
7. S. Mallat, *A wavelet tour of signal processing*, Academic Press, Great Britain, 1998.
8. P. Wong, "Adaptive error diffusion and its application in multiresolutional rendering, *IEEE Trans. on Image Proc.* **5**(7), pp. 1184–1196, 1996.
9. P. W. J.R. Goldschneider, E. Riskin, "Embedded multilevel error diffusion, *IEEE Transactions on Image Processing* **6**, pp. 956–964, July 1997.
10. N. A. Breaux and C. H. Chu, "Wavelet methods for compression, rendering, and descreening in digital halftoning, *Proc. of SPIE* **3078**, pp. 656–667, April 1997.
11. E. Peli, "Multiresolution error-convergence halftone algorithm, *Journal of the Optical Society of America A* **8**, pp. 625–636, April 1991.
12. M. Gupta, M. Gormish, and D. G. Stork, "Block color quantization: a new method for halftoning, *IEEE Intl. Conf. on Image. Proc.* **3**, pp. 460–463, 2000.
13. I. Katsavoundidis and C. Kuo, "A recursive multiscale error-diffusion technique for digital halftoning, *Proc. of SPIE* **2094**, pp. 487–498, 1993.
14. I. Katsavoundidis and C. Kuo, "A multiscale error diffusion technique for digital halftoning, *IEEE Trans. on Image Proc.* **6**, pp. 483–490, March 1997.
15. H. Szu, Y. Zhang, M. Sun, and C. Li, "Neural network adaptive digital image screen halftoning (dish) based on wavelet transform preprocessing, *Proc. of the SPIE* **2242**, pp. 963–966, 1994.
16. X. Zhang, D. Silverstein, J. Farrell, and B. Wandell, "Color image quality metric s-cielab and its application on halftone texture visibility, *Proceedings of the IEEE CompCon* , 1997.
17. B. Wandell, www.stanford.edu/~wandell. This web page has links to papers and code for sCIElab metric.
18. R. Floyd and L. Steinberg, "An adaptive algorithm for spatial greyscale, *Proceedings of the Society for Information Display* **17**(2), pp. 75–77, 1976.
19. H. Inose and Y. Yasuda, "A unity bit coding method by negative feedback, *Proceedings of the IEEE* **51**, pp. 1524–1535, 1963.